Upper limits on the Peccei-Quinn scale and on the reheating temperature in axino dark matter scenarios

Freitas, A ; Steffen, F D ; Tajuddin, N ; Wyler, D

Abstract: Considering axino cold dark matter scenarios with a long-lived charged slepton, we study constraints on the Peccei–Quinn scale fa and on the reheating temperature TR imposed by the dark matter density and by big bang nucleosynthesis (BBN). For an axino mass compatible with large-scale structure, View the MathML source, temperatures above 109 GeV become viable for fa>3×1012 GeV. We calculate the slepton lifetime in hadronic axion models. With the dominant decay mode being two-loop suppressed, this lifetime can be sufficiently large to allow for primordial bound states leading to catalyzed BBN of lithium-6 and beryllium-9. This implies new upper limits on fa and on TR that depend on quantities which will be probed at the Large Hadron Collider.

DOI: https://doi.org/10.1016/j.physletb.2009.07.047

MPP–2009–12, ZU–TH 06/09

Upper Limits on the Peccei–Quinn Scale and on the Reheating Temperature in Axino Dark Matter Scenarios

Ayres Freitas,[1,*] Frank Daniel Steffen,[2,†] Nurhana Tajuddin,[3,‡] and Daniel Wyler[3,§]

[1] *Department of Physics and Astronomy, University of Pittsburgh, PA 15260, USA*
[2] *Max-Planck-Institut für Physik, Föhringer Ring 6, D–80805 Munich, Germany*
[3] *Institut für Theoretische Physik, Universität Zürich, Winterthurerstrasse 190, CH–8057 Zürich, Switzerland*

Considering axino cold dark matter scenarios with a long-lived charged slepton, we study constraints on the Peccei–Quinn scale f_a and on the reheating temperature $T_{\rm R}$ imposed by the dark matter density and by big bang nucleosynthesis (BBN). For an axino mass compatible with large-scale structure, $m_{\widetilde{a}} \gtrsim 100$ keV, temperatures above 10^9 GeV become viable for $f_a > 3 \times 10^{12}$ GeV. We calculate the slepton lifetime in hadronic axion models. With the dominant decay mode being two-loop suppressed, this lifetime can be sufficiently large to allow for primordial bound states leading to catalyzed BBN of Lithium–6 and Beryllium–9. This implies new upper limits on f_a and on $T_{\rm R}$ that depend on quantities which will be probed at the Large Hadron Collider.

PACS numbers: 98.80.Cq, 95.35.+d, 12.60.Jv, 95.30.Cq

I. INTRODUCTION

In supersymmetric (SUSY) extensions of the Standard Model with conserved R-parity, the lightest supersymmetric particle (LSP) is stable and thus a compelling dark matter candidate. While the lightest neutralino $\widetilde{\chi}_1^0$ or the gravitino $\widetilde{G}$ are often considered to be the LSP, the axino $\widetilde{a}$ is also a well-motivated LSP candidate and hence an equally compelling dark matter candidate [1, 2, 3, 4, 5, 6, 7] beyond the minimal supersymmetric Standard Model (MSSM).

The axino $\widetilde{a}$ is the fermionic partner of the axion in SUSY extensions of the Standard Model in which the Peccei–Quinn (PQ) mechanism is embedded as a solution of the strong CP problem. Because its interactions are suppressed by the PQ scale $f_a \gtrsim 6\times10^8$ GeV [8, 9, 10, 11], the axino can be classified as an extremely weakly interacting particle (EWIP). With the axino being the LSP, the lightest Standard Model superpartner or lightest ordinary superpartner (LOSP) is unstable and can thus be an electrically charged particle such as a charged slepton $\tilde{l}_1$. For example, the lighter stau $\widetilde{\tau}_1$—which is the superpartner of the tau lepton τ—is the LOSP in a large part of the parameter space of the constrained MSSM (CMSSM). Due to the extremely suppressed axino interaction strength, such an LOSP would be long-lived and would appear as a quasi-stable charged particle in the collider detectors. Its ultimate decay into the $\widetilde{a}$ LSP will often occur outside of those detectors. Some decays however may be accessible experimentally and may allow one to probe the PQ scale at colliders [12]. While an axino LSP identification [12] will require challenging experimental setups [13], quasi-stable $\tilde{l}_1$'s can appear as a first hint for the existence of SUSY and of the axino LSP at the Large Hadron Collider (LHC) already within the next three years.

In this Letter we focus on the axino LSP case with a long-lived $\tilde{l}_1$ LOSP and in particular on scenarios in which the axino provides the dominant contribution to the dark matter density [14]

$$\Omega_{\rm dm}^{3\sigma} h^2 = 0.105^{+0.021}_{-0.030} \qquad (1)$$

with $h = 0.73^{+0.04}_{-0.03}$ denoting the Hubble constant in units of 100 km Mpc^{-1}s^{-1}. The 3σ range indicated rests on a representative six-parameter "vanilla" model.

The thermally produced (TP) axino density $\Omega_{\widetilde{a}}^{\rm TP}$ must not exceed $\Omega_{\rm dm}$. This puts upper limits on the post-inflationary reheating temperature $T_{\rm R}$ [3, 5, 7, 15, 16]. These $T_{\rm R}$ limits—which depend on the axino mass $m_{\widetilde{a}}$ and on the PQ scale f_a—can be very restrictive for models of inflation and of baryogenesis. For example, $T_{\rm R} \lesssim 10^6$ GeV is found for $f_a = 10^{11}$ GeV and $m_{\widetilde{a}} = 100$ keV [5]. Indeed, for $m_{\widetilde{a}} \gtrsim 100$ keV, temperatures above 10^9 GeV can become viable only for larger values of the PQ scale, $f_a \gtrsim 3 \times 10^{12}$ GeV, if a standard thermal history is assumed.[1] While $T_{\rm R} \gtrsim 10^9$ GeV is required, e.g., by standard thermal leptogenesis with hierarchical right-handed neutrinos [21, 22, 23, 24, 25], we show in this work that $f_a \gtrsim 3 \times 10^{12}$ GeV can be associated with restrictive BBN constraints due to the

*Electronic address: afreitas@pitt.edu
†Electronic address: steffen@mppmu.mpg.de
‡Electronic address: nurhana@physik.uzh.ch
§Electronic address: wyler@physik.unizh.ch

[1] Depending on the model, the saxion—which is the bosonic partner of the axino that appears in addition to the axion—can be a late decaying particle and as such be associated with significant entropy production [17, 18, 19, 20]. This could affect cosmological constraints [16] including those considered in this work. Leaving a study of saxion effects for future work, we assume in this Letter a standard thermal history and thereby that those effects are negligible.

long-lived $\tilde{l}_1$ LOSP and its potential to form primordial bound states. In fact, we find that those BBN constraints imply upper limits on f_a and thereby new upper limits on $T_{\rm R}$.

We consider hadronic (or KSVZ) axion models [26, 27] in a SUSY setting [28]. In this class of models, the axino couples to the MSSM particles only indirectly through loops of heavy KSVZ (s)quarks. Thereby, the dominant 2-body decay of the $\tilde{l}_1$ LOSP into the associated lepton and the axino is described in leading order by 2-loop diagrams [4, 12]. Using a heavy mass expansion, we evaluate the 2-loop diagrams explicitly and obtain the decay width that governs the $\tilde{l}_1$ lifetime $\tau_{\tilde{l}_1}$. For a given thermal freeze-out yield of negatively charged $\tilde{l}_1^-$'s, $Y_{\tilde{l}_1^-}$, our $\tau_{\tilde{l}_1}$ result allows us to infer the BBN constraints associated with primordial ^{6}Li and ^{9}Be production that can be catalyzed by $\tilde{l}_1^-$-nucleus-bound-state formation [29, 30, 31]. While BBN constraints were often assumed to play only a minor role in the axino LSP case, we explore the ones from bound-state effects explicitly and show that they impose new restrictive limits on f_a and $T_{\rm R}$.

Before proceeding, let us comment on axion physics. We assume a cosmological scenario in which the spontaneous breaking of the PQ symmetry occurs before inflation leading to $T_{\rm R} < f_a$ so that no PQ symmetry restoration takes place during inflation or in the course of reheating. Since axions are never in thermal equilibrium for the large f_a values considered, their relic density Ω_a is governed by the initial misalignment angle Θ_i of the axion field with respect to the CP-conserving position; cf. [6, 9, 32] and references therein. With a sufficiently small Θ_i being an option, $\Omega_a \ll \Omega_{\rm dm}$ is possible even for f_a as large as $10^{14}\,$GeV. We assume $\Omega_a \ll \Omega_{\rm dm}$ to keep the presented constraints conservative.

The remainder of this Letter is organized as follows. In the next section we review the upper limits on $T_{\rm R}$ imposed by $\Omega_{\tilde{a}}^{\rm TP} \leq \Omega_{\rm dm}$ which provide our motivation to consider $f_a \gtrsim 3 \times 10^{12}$ GeV. Section III presents the results for the $\tilde{l}_1$ NLSP lifetime obtained from our 2-loop calculation. Section IV explores the BBN constraints from $\tilde{l}_1$-nucleus-bound-state formation. In Sect. V, we show that those BBN constraints imply new $T_{\rm R}$ limits if the considered axino LSP scenario is realized in nature. Analytic expressions that approximate the obtained limits in a conservative way are derived in Sect. VI.

II. CONSTRAINTS ON $T_{\rm R}$

Because of their extremely weak interactions, the temperature $T_{\rm f}$ at which axinos decouple from the thermal plasma in the early Universe can be very high, e.g., $T_{\rm f} \gtrsim 10^9\,$GeV for $f_a \gtrsim 10^{11}\,$GeV [5, 33] or $T_{\rm f} \gtrsim 10^{11}\,$GeV for $f_a \gtrsim 10^{12}\,$GeV [5]. Accordingly, axinos decouple as a relativistic species in scenarios with $T_{\rm R} > T_{\rm f}$. The resulting relic density is then insensitive to the precise value of $T_{\rm R}$ [33]: $\Omega_{\tilde{a}}^{\rm therm} h^2 \simeq m_{\tilde{a}}/(2\text{ keV})$. Moreover, $\Omega_{\tilde{a}}^{\rm therm} \leq \Omega_{\rm dm}$ implies $m_{\tilde{a}} \lesssim 0.2$ keV. For a scenario with $\Omega_{\tilde{a}}^{\rm therm} \simeq \Omega_{\rm dm}$, this is in conflict with large-scale structure which requires a smaller present free-streaming velocity of axino dark matter and thereby $m_{\tilde{a}} \gtrsim 1$ keV; cf. Sect. 5.2 and Table 1 of Ref. [34]. Focussing on scenarios in which axinos provide the dominant component of cold dark matter with a negligible present free-streaming velocity, $m_{\tilde{a}} \gtrsim 100$ keV, we thus assume $T_{\rm R} < T_{\rm f}$ in the remainder of this work.

In scenarios with $T_{\rm R} < T_{\rm f}$, axino dark matter can be produced efficiently in scattering processes of particles that are in thermal equilibrium within the hot MSSM plasma [3, 5, 35, 36]. The efficiency of this thermal axino production is sensitive to $T_{\rm R}$ and f_a and the associated relic density reads [5][2]

$$\Omega_{\tilde{a}}^{\rm TP} h^2 \simeq 5.5\, g_{\rm s}^6(T_{\rm R}) \ln\left(\frac{1.211}{g_{\rm s}(T_{\rm R})}\right)\left(\frac{10^{11}\,\text{GeV}}{f_a}\right)^2 \times \left(\frac{m_{\tilde{a}}}{0.1\text{ MeV}}\right)\left(\frac{T_R}{10^7\,\text{GeV}}\right) \quad (2)$$

with the strong coupling $g_{\rm s}$ and the axion-model-dependent color anomaly of the PQ symmetry absorbed into f_a.[3] Using hard thermal loop (HTL) resummation together with the Braaten-Yuan prescription [38], this expression has been derived within SUSY QCD in a consistent gauge-invariant treatment that requires weak couplings $g_{\rm s}(T_{\rm R}) \ll 1$ and thus high temperatures. Accordingly, (2) is most reliable for $T \gg 10^4\,$GeV [5].[4] Note that we evaluate $g_s(T_{\rm R}) = \sqrt{4\pi\alpha_s(T_{\rm R})}$ according to its 1-loop renormalization group running within the MSSM from $\alpha_s(m_{\rm Z}) = 0.1176$ at $m_{\rm Z} = 91.1876$ GeV.

In Fig. 1, $(m_{\tilde{a}}, T_{\rm R})$ regions in which the thermally produced axino density (2) is within the nominal 3σ range (1) are indicated for f_a values between $10^{11}\,$GeV and $10^{14}\,$GeV by gray bands (as labeled). For given values of $m_{\tilde{a}}$ and f_a, $T_{\rm R}$ values above the corresponding band are disfavored by $\Omega_{\tilde{a}}^{\rm TP} > \Omega_{\rm dm}$; see also [3, 5, 7, 15, 16]. From (2) and Fig. 1, one can see that the viability of temperatures above $10^9\,$GeV points to $f_a > 3\times10^{12}\,$GeV if one insists on cold axino dark matter, $m_{\tilde{a}} \gtrsim 100$ keV, providing the dominant component of $\Omega_{\rm dm}$. Those f_a values and $m_{\tilde{a}} \lesssim 1$ GeV are thereby favored by the viability of standard thermal leptogenesis with hierarchical right-handed neutrinos [21, 22, 23, 24, 25].

---

[2] We refer to $T_{\rm R}$ as the initial temperature of the radiation-dominated epoch. Relations to $T_{\rm R}$ definitions in terms of the decay width of the inflaton field can be established in the way presented explicitly for the $\widetilde{G}$ LSP case in Ref. [37].

[3] For the hadronic axion models considered below, the color anomaly is $N = 1$ so that (2) applies directly, i.e., without the need to absorb N into the definition of f_a.

[4] For thermal axino production at lower temperatures, cf. [36].

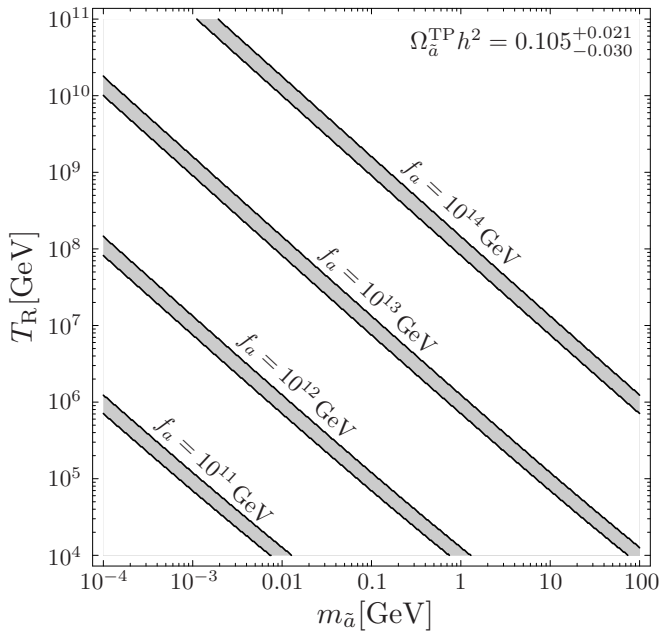

FIG. 1: Upper limits on the reheating temperature $T_{\rm R}$ as a function of the axino mass $m_{\tilde{a}}$ in scenarios with axino cold dark matter for $f_a = 10^{11}$, 10^{12}, 10^{13}, and 10^{14} GeV (as labeled). For $(m_{\tilde{a}}, T_{\rm R})$ combinations within the gray bands, the thermally produced axino density $\Omega_{\tilde{a}}^{\rm TP}h^2$ is within the nominal 3σ range (1). For given f_a, the region above the associated band is disfavored by $\Omega_{\tilde{a}}^{\rm TP}h^2 > 0.126$.

III. THE CHARGED SLEPTON LOSP CASE

While the $T_{\rm R}$ limits discussed above are independent of the LOSP, we turn now to the phenomenologically attractive case in which the LOSP is a charged slepton $\tilde{l}_1$. To be specific, we focus on the $\tilde{\tau}_1$ LOSP case under the simplifying assumption that the lighter stau is purely 'right-handed,' $\tilde{\tau}_1 = \tilde{\tau}_{\rm R}$, which is a good approximation at least for small $\tan\beta$. The $\widetilde{\chi}_1^0$–$\tilde{\tau}_1$ coupling is then dominated by the bino coupling. For further simplicity, we also assume that the lightest neutralino is a pure bino: $\widetilde{\chi}_1^0 = \widetilde{B}$.

We consider SUSY hadronic axion models in which the interaction of the axion multiplet Φ with the heavy KSVZ quark multiplets Q_1 and Q_2 is described by the superpotential

$$W_{\rm PQ} = y\Phi Q_1 Q_2 \tag{3}$$

with the quantum numbers given in Table I and the Yukawa coupling y. From the 2-component fields of Table I, the 4-component fields describing the axino and the heavy KSVZ quark are given, respectively, by

$$\widetilde{a} = \begin{pmatrix} \chi \\ \bar{\chi} \end{pmatrix} \quad \text{and} \quad Q = \begin{pmatrix} q_1 \\ \bar{q}_2 \end{pmatrix} \ . \tag{4}$$

For the heavy KSVZ (s)quark masses, we use the SUSY limit $M_{\widetilde{Q}_{1,2}} = M_Q = y\langle\phi\rangle = yf_a/\sqrt{2}$ with both y and f_a taken to be real by field redefinitions. The phenomenological constraint $f_a \gtrsim 6\times10^8$ GeV [8, 9, 10, 11] thus implies a large mass hierarchy between the KSVZ (s)quarks and the weak and the soft SUSY mass scales for $y = \mathcal{O}(1)$,

$$M_{\widetilde{Q}_{1,2}}, M_Q \gg m_{\rm Z}, m_{\rm SUSY} \ . \tag{5}$$

TABLE I: The axion multiplet Φ, the heavy KSVZ quark multiplets $Q_{1,2}$, and the associated quantum numbers considered in this work.

chiral multiplet	$\rm U(1)_{PQ}$	$(\rm SU(3)_c, SU(2)_L)_Y$
$\Phi = \phi + \sqrt{2}\chi\theta + F_\Phi\theta\theta$	+1	$(\mathbf{1},\mathbf{1})_0$
$Q_1 = \widetilde{Q}_1 + \sqrt{2}q_1\theta + F_1\theta\theta$	-1/2	$(\mathbf{3},\mathbf{1})_{+e_Q}$
$Q_2 = \widetilde{Q}_2 + \sqrt{2}q_2\theta + F_2\theta\theta$	-1/2	$(\mathbf{3}^*,\mathbf{1})_{-e_Q}$

In R-parity conserving settings in which the $\tilde{\tau}_{\rm R}$ LOSP is the NLSP, its lifetime $\tau_{\tilde{\tau}}$ is governed by the decay $\tilde{\tau}_{\rm R} \to \tau\tilde{a}$. For the models given by (3) and Table I, the Feynman diagrams of the dominant contributions to the 2-body stau NLSP decay $\tilde{\tau}_{\rm R} \to \tau\tilde{a}$ are shown in Fig. 2. Since $m_\tau \ll m_{\tilde{\tau}}$, we work in the limit $m_\tau \to 0$. In the

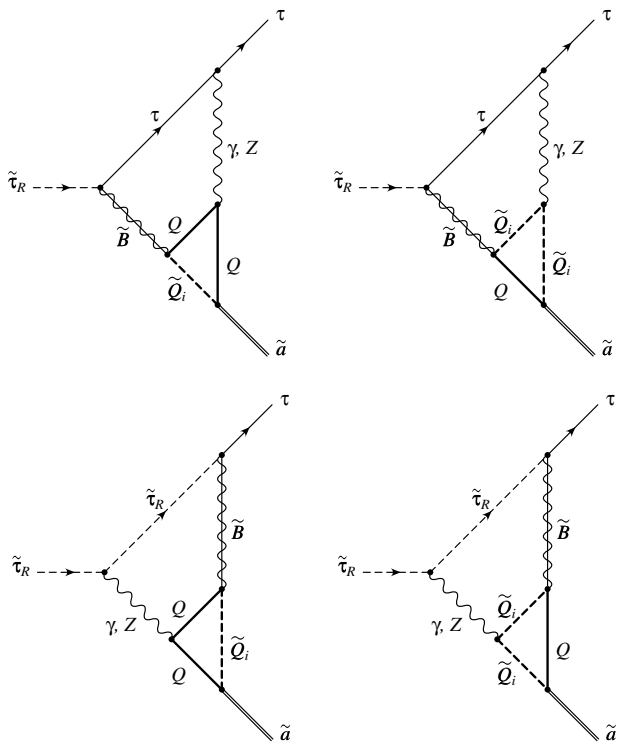

FIG. 2: Feynman diagrams of the dominant contributions to the stau NLSP decay $\tilde{\tau}_{\rm R} \to \tau\tilde{a}$ in a SUSY hadronic axion model with one KSVZ quark $Q = (q_1, \bar{q}_2)^{\rm T}$ and the associated squarks $\widetilde{Q}_{1,2}$. The considered quantum numbers are given in Table I. For simplicity, the lightest neutralino is assumed to be a pure bino $\widetilde{\chi}_1^0 = \widetilde{B}$ and the tau mass is neglected.

calculation of the 2-loop diagrams, the hierarchy (5) allows us to make use of a heavy mass expansion in powers of $1/f_a$. In this asymptotic expansion, it is sufficient to calculate the leading term of the amplitude $\propto 1/f_a$ since the sub-leading terms ($\propto 1/f_a^2$) are suppressed by many orders of magnitude. Details of this calculation and the full result of the leading term will be presented in a forthcoming publication [39]. The dominant leading logarithmic (LL) part of the partial width is given by

$$\Gamma_{\rm tot}^{\widetilde{\tau}_{\rm R}} \approx \Gamma(\widetilde{\tau}_{\rm R} \to \tau \widetilde{a})_{\rm LL} \tag{6}$$

$$= \frac{81\,\alpha^4 e_Q^4}{128\pi^5 \cos^8\theta_W} \frac{m_{\widetilde{\tau}}\, m_{\widetilde{B}}^2}{f_a^2} \left(1 - \frac{m_{\widetilde{a}}^2}{m_{\widetilde{\tau}}^2}\right)^2 \ln^2\left(\frac{y f_a}{\sqrt{2} m_{\widetilde{\tau}}}\right), \tag{7}$$

where α denotes the fine structure constant, $m_{\widetilde{B}}$ the bino mass, and θ_W the weak mixing angle.[5] However, all numerical results shown in the plots below rest on the full calculation.[6]

In Fig. 3 our result of the full leading term for $1/\Gamma(\widetilde{\tau}_{\rm R} \to \tau\,\widetilde{a}) \approx \tau_{\widetilde{\tau}}$ and its relation to $m_{\widetilde{\tau}}$ is illustrated for $m_{\widetilde{a}}^2/m_{\widetilde{\tau}}^2 \ll 1$, $m_{\widetilde{B}} = 1.1\, m_{\widetilde{\tau}}$, $|e_Q| = 1/3$, and $y = 1$. The considered f_a values are between 10^{10} and 10^{14} GeV.

The results show that $\Gamma(\widetilde{\tau}_{\rm R} \to \tau\,\widetilde{a})$ is largely governed by the LL part (7). Comparing equation (7) with the full expression [39] (see also Fig. 3), we estimate that it gives the total width $\Gamma_{\rm tot}^{\widetilde{\tau}_{\rm R}}$ and thereby the $\widetilde{\tau}_{\rm R}$ lifetime $\tau_{\widetilde{\tau}} = 1/\Gamma_{\rm tot}^{\widetilde{\tau}_{\rm R}}$ to within 10% to maximally 15%, depending on the values of f_a and $m_{\widetilde{\tau}}$.

One can see that $f_a \gtrsim 10^{12}$ GeV is associated with $\tau_{\widetilde{\tau}} > 1$ s for $m_{\widetilde{\tau}} \lesssim 1$ TeV, i.e., for the $m_{\widetilde{\tau}}$ range that would be accessible at the LHC. Accordingly, BBN constraints on axino LSP scenarios with the stau NLSP can become important as will be discussed explicitly below. Note that not only the LL part (7) but the full leading term is strongly sensitive to the electric charge of the heavy KSVZ fields: $\Gamma(\widetilde{\tau}_{\rm R} \to \tau\,\widetilde{a}) \propto e_Q^4$. With respect to the case in Fig. 3, $\tau_{\widetilde{\tau}}$ is thus reduced by a factor of 81 (16) for $|e_Q| = 1$ (2/3). On the other hand, if $e_Q = 0$, the decay of the $\widetilde{\tau}$ NLSP will require 4-loop diagrams involving gluons, gluinos, and ordinary (s)quarks, which would thus lead to significantly larger lifetimes than in Fig. 3.

Let us compare our result with the one for $\Gamma(\widetilde{\tau}_{\rm R} \to \tau\,\widetilde{a})$ that had been obtained in [12] with an effective theory in which the heavy KSVZ (s)quark loop was integrated out,

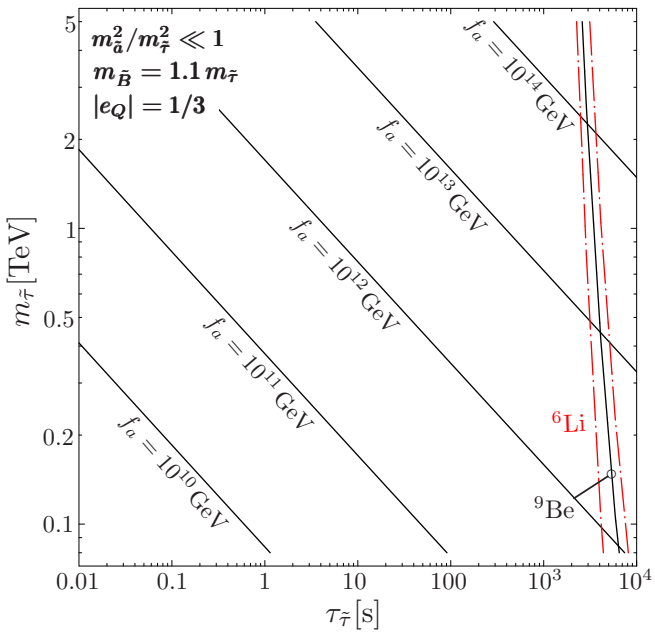

FIG. 3: The lifetime of the $\widetilde{\tau}_{\rm R}$ NLSP, $1/\Gamma(\widetilde{\tau}_{\rm R} \to \tau\,\widetilde{a}) \approx \tau_{\widetilde{\tau}}$ in relation to its mass $m_{\widetilde{\tau}}$ for $m_{\widetilde{a}}^2/m_{\widetilde{\tau}}^2 \ll 1$, $m_{\widetilde{B}} = 1.1\, m_{\widetilde{\tau}}$, $|e_Q| = 1/3$, $y = 1$, and f_a values from 10^{10} to 10^{14} GeV. For a stau yield $Y_{\widetilde{\tau}}$ given by (8), $\tau_{\widetilde{\tau}}$ values to the right of the nearly vertical solid and dash-dotted (red) lines are disfavored by the constraints (14) and (13) on catalyzed BBN (CBBN) of ^{9}Be and ^{6}Li, respectively [31]; see Sect. IV for details.

i.e., by using the method described in [41]. There, the logarithmic divergencies were regulated with the cut-off f_a, and only dominant contributions were kept. While the dependence on the quantum numbers of the KSVZ (s)quarks was absorbed into the constant $C_{\rm aYY}$, the uncertainty associated with this cut-off procedure was expressed in terms of a mass scale m and a factor ξ in Ref. [12]. Our 2-loop calculation allows us to eliminate this uncertainty. In particular, we find from (7) that one must set $C_{\rm aYY} = 6e_Q^2$, $\xi = 1$, and $m = \sqrt{2} m_{\widetilde{\tau}}/y$. This shows how important the full 2-loop calculation is; had one, for instance, set the scale m to M_Z, a deviation of up to about 45% would result at $m_{\widetilde{\tau}} = 1$ TeV. Furthermore, the non-LL part can account, as mentioned, for up to 15% of the decay rate.

In the early Universe, the stau LOSP decouples as a WIMP before its decay into the axino LSP. The thermal relic stau abundance prior to decay then depends on details of the SUSY model such as the mass splitting among the lightest Standard Model superpartners [42] or the left-right mixing of the stau LOSP [43, 44]. However, focussing on the $\widetilde{\tau}_{\rm R}$ LOSP setting, we work with the typical thermal freeze out yield described by

$$Y_{\widetilde{\tau}} \equiv \frac{n_{\widetilde{\tau}_{\rm R}}}{s} = 2 Y_{\widetilde{\tau}_{\rm R}^-} \simeq 0.7 \times 10^{-12} \left(\frac{m_{\widetilde{l}_1}}{1\ {\rm TeV}}\right), \tag{8}$$

where s denotes the entropy density and $n_{\widetilde{\tau}_{\rm R}}$ the total $\widetilde{\tau}_{\rm R}$ number density for an equal number density of positively

[5] We use $\alpha = \alpha^{\overline{\rm MS}}(m_{\rm Z}) = 1/129$ [40] and $\sin^2\theta_W = 1 - m_W^2/m_Z^2 = 0.2221$.

[6] Note that the 3-body decay $\widetilde{\tau}_{\rm R} \to \tau\widetilde{a}\gamma$ occurs already at the 1-loop level. The corresponding amplitude however is not enhanced by $\ln(y f_a/\sqrt{2} m_{\widetilde{\tau}})$ which can be as large as 20.4–27.3 for $m_{\widetilde{\tau}}/y = 100$ GeV and $f_a = 10^{11}$–10^{14} GeV. In fact, the branching ratio of $\widetilde{\tau}_{\rm R} \to \tau\widetilde{a}\gamma$ stays below about 3% once both the energy of the photon E_γ and its opening angle θ with respect to the τ direction are required to be not too small. Those cuts are needed because of an infrared and a collinear divergence for $E_\gamma \to 0$ and $\theta \to 0$, respectively, which would be canceled by the virtual 3-loop correction to the 2-body decay channel [39].

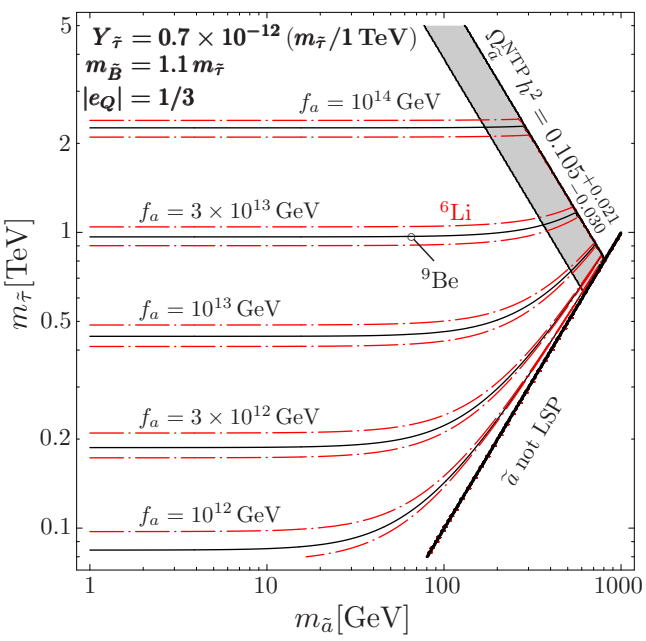

FIG. 4: Cosmological constraints on the masses of the $\widetilde a$ LSP and the $\widetilde\tau_{\rm R}$ NLSP for $Y_{\tilde\tau}$ given by (8). The gray band indicates where $\Omega_{\tilde a}^{\rm NTP}h^2$ lies within the region (1). Above this band, $\Omega_{\tilde a}^{\rm NTP}h^2 > 0.126$. Because of the CBBN reactions (10)–(12) becoming efficient, the regions below the solid and the dash-dotted (red) lines are disfavored by the observationally inferred limits on primordial ^{9}Be (14) and ^{6}Li (13), respectively, for f_a as indicated, $m_{\widetilde B} = 1.1\,m_{\tilde\tau}$, $|e_Q| = 1/3$, and $y = 1$. The shown CBBN constraints thus provide upper limits on f_a as a function of $m_{\tilde a}$ and $m_{\tilde\tau}$. Focussing on the $\widetilde a$ LSP case, we do not consider the region in which $m_{\tilde a} > m_{\tilde\tau}$.

and negatively charged $\widetilde\tau_{\rm R}$'s. This approximation (8) agrees with the curve in Fig. 1 of Ref. [42] derived for $m_{\widetilde B} = 1.1\,m_{\tilde\tau}$ and for $m_{\tilde\tau}$ significantly below the masses of the lighter selectron and the lighter smuon.

Since each stau NLSP decays into one axino LSP, the thermal relic stau abundance leads to a non-thermally produced (NTP) axino density [1, 2, 3, 4]

$$\Omega_{\tilde a}^{\rm NTP}h^2 = m_{\tilde a}\,Y_{\tilde\tau}\,s(T_0)h^2/\rho_{\rm c}\ , \tag{9}$$

where $\rho_{\rm c}/[s(T_0)h^2] = 3.6\times10^{-9}\,\mathrm{GeV}$ [8]. For $Y_{\tilde\tau}$ given by (8), $\Omega_{\tilde a}^{\rm NTP}h^2$ is within the nominal 3σ range (1) for $(m_{\tilde a}, m_{\tilde\tau})$ combinations indicated by the gray band in Fig. 4. While $m_{\tilde\tau}$ values above this band are disfavored by $\Omega_{\tilde a}^{\rm NTP} > \Omega_{\rm dm}$, $\Omega_{\tilde a}^{\rm NTP}$ is only a minor fraction ($\lesssim 1\%$) of $\Omega_{\rm dm}$ for $m_{\tilde a} \lesssim 1$ GeV and $m_{\tilde\tau} \lesssim 5$ TeV. For $m_{\tilde a} \lesssim 1$ GeV, the $T_{\rm R}$ limits shown in Fig. 1 will thus shift only marginally by taking $\Omega_{\tilde a}^{\rm NTP}$ into account.

IV. CBBN CONSTRAINTS

The presence of negatively charged $\widetilde\tau_{\rm R}^-$'s at cosmic times of $t > 10^3$ s can allow for primordial ^{6}Li and ^{9}Be production via the formation of $(^4\mathrm{He}\,\widetilde\tau_{\rm R}^-)$ and $(^8\mathrm{Be}\,\widetilde\tau_{\rm R}^-)$ bound states. Indeed, depending on the lifetime $\tau_{\tilde\tau}$ and the abundance $Y_{\widetilde\tau_{\rm R}^-} = Y_{\tilde\tau}/2$, the following catalyzed BBN (CBBN) reactions can become efficient [29, 30, 31][7]

$$(^4\mathrm{He}\,\widetilde\tau_{\rm R}^-) + \mathrm{D} \ \rightarrow\ {}^6\mathrm{Li} + \widetilde\tau_{\rm R}^- \tag{10}$$

$$^4\mathrm{He} + (^4\mathrm{He}\,\widetilde\tau_{\rm R}^-) \ \rightarrow\ (^8\mathrm{Be}\,\widetilde\tau_{\rm R}^-) + \gamma \tag{11}$$

$$(^8\mathrm{Be}\,\widetilde\tau_{\rm R}^-) + n \ \rightarrow\ {}^9\mathrm{Be} + \widetilde\tau_{\rm R}^-\ . \tag{12}$$

Observationally inferred limits on the primordial abundances of both ^{6}Li and ^{9}Be can thus be used to extract $\tau_{\tilde\tau}$-dependent upper bounds on $Y_{\widetilde\tau_{\rm R}^-}$. In this Letter, we adopt those bounds directly from Fig. 5 of Ref. [31] relying on observationally inferred limits on the primordial fractions of ^{6}Li [46, 47, 48] and ^{9}Be [31] of respectively

$$^6\mathrm{Li/H}|_{\rm obs} \ \leq\ 10^{-11}\text{–}10^{-10}\ , \tag{13}$$

$$^9\mathrm{Be/H}|_{\rm obs} \ \leq\ 2.1\times10^{-13}\ . \tag{14}$$

Confronting the $\tau_{\tilde\tau}$-dependent $Y_{\widetilde\tau_{\rm R}^-}$ bounds with (8), we obtain the CBBN constraints shown in Figs. 3 and 4 by the solid (^{9}Be) lines and by pairs of dash-dotted (^{6}Li, red) lines associated, respectively, with (14) and the range in (13). The regions to the right of the corresponding lines in Fig. 3 and the ones below the corresponding lines in Fig. 4 are disfavored by CBBN due to an excess of ^{9}Be and ^{6}Li over the given limits.

In Fig. 4, f_a values from 10^{12} up to 10^{14} GeV are considered for $m_{\widetilde B} = 1.1\,m_{\tilde\tau}$, $|e_Q| = 1/3$, and $y = 1$. For $f_a \lesssim 10^{12}$ GeV and $m_{\tilde a}^2/m_{\tilde\tau}^2 \ll 1$, the $m_{\tilde\tau}$ values disfavored by CBBN are already excluded by the limit $m_{\tilde\tau} \gtrsim 80$ GeV [8] from searches for long-lived staus at the Large Electron Positron (LEP) collider; see also Fig. 3. Thus, for $f_a < 10^{12}$ GeV and $m_{\tilde\tau} \gtrsim 80$ GeV, CBBN constraints can only be effective if $m_{\tilde a}$ and $m_{\tilde\tau}$ are degenerate leading to a significant phase space suppression resulting in $\tau_{\tilde\tau} > 10^3$ s. For $|e_Q| = 1$, the CBBN constraints agree basically with the contours shown in Fig. 4 but with f_a values shifted upwards by one order of magnitude.

The CBBN constraints follow contours of constant $\tau_{\tilde\tau}$. Indeed, for $m_{\tilde a}^2/m_{\tilde\tau}^2 \ll 1$, the CBBN constraints also become independent of $m_{\tilde a}$. Moreover, for given f_a, $m_{\tilde a}$, and $m_{\tilde\tau}$, larger values of $\tau_{\tilde\tau}$ and thereby more restrictive CBBN constraints are encountered at smaller values of e_Q, $m_{\widetilde B}$, or y. By decreasing $m_{\widetilde B}$ towards $m_{\tilde\tau}$, the CBBN constraints become more restrictive because of both a larger $\tau_{\tilde\tau}$ and a yield $Y_{\tilde\tau}$ that is enhanced by stau–bino coannihilation. However, the effect is dominated by the change in $\tau_{\tilde\tau}$ due to the relatively mild impact of $Y_{\widetilde\tau_{\rm R}^-}$ on the CBBN processes in the relevant region; see Fig. 5 of Ref. [31].

[7] The large ^{9}Be-production cross section reported and used in Refs. [30, 31] has recently been questioned by Ref. [45], in which a study based on a four-body model is announced as work in progress to clarify the efficiency of ^{9}Be production.

Let us stress that each set of CBBN constraints in Fig. 4—such as the ^{9}Be contours—imposes an upper limit on the PQ scale f_a as a function of $m_{\widetilde{a}}$ and $m_{\widetilde{\tau}}$. Since those f_a limits become only more restrictive for $m_{\widetilde{a}} \to m_{\widetilde{\tau}}$, their $m_{\widetilde{a}}$-independent values at $m_{\widetilde{a}}^2/m_{\widetilde{\tau}}^2 \ll 1$ are conservative limits. In the considered $\widetilde{a}$ LSP case, those are relevant for studies and searches of axions even without further insights into $m_{\widetilde{a}}$.

V. PROBING $T_{\rm R}$ WITH BBN AND AT COLLIDERS

If the considered $\widetilde{a}$ LSP scenario is realized in nature with not too heavy Standard Model superpartners, one will be able to measure $m_{\widetilde{\tau}}$ and $m_{\widetilde{B}}$ at the LHC. Moreover, with further experimental insights into the SUSY model, $Y_{\widetilde{\tau}}$ can be calculated for a standard cosmological history with $T_{\rm R}$ above the temperature at which the stau decouples from the primordial plasma. For concreteness, let us assume that $m_{\widetilde{B}} = 1.1\, m_{\widetilde{\tau}}$ and that the resulting yield agrees with (8). The measured $m_{\widetilde{\tau}}$ value can then be confronted with the CBBN constraints shown in Figs. 3 and 4. For $m_{\widetilde{\tau}} = 500$ GeV, for example, the CBBN constraints imply $f_a \lesssim 10^{13}$ GeV for $m_{\widetilde{a}}^2/m_{\widetilde{\tau}}^2 \ll 1$, $|e_Q| = 1/3$, and $y = 1$. Then $T_{\rm R} \gtrsim 10^9$ GeV—as required by standard thermal leptogenesis—will only be viable for $m_{\widetilde{a}} \lesssim 1$ MeV; cf. Fig. 1. While $\tau_{\widetilde{\tau}}$ is practically independent of such a small $m_{\widetilde{a}}$, one could in principle test this $m_{\widetilde{a}}$ limit from the kinematics of the 2-body decay $\widetilde{\tau}_{\rm R} \to \tau \widetilde{a}$ [12], i.e., from a measurement of the energy of the emitted tau E_τ,

$$m_{\widetilde{a}} = \sqrt{m_{\widetilde{\tau}}^2 + m_\tau^2 - 2 m_{\widetilde{\tau}} E_\tau}\ . \tag{15}$$

At present, however, this seems to be a realistic option only for $0.1 m_{\widetilde{\tau}} \lesssim m_{\widetilde{a}} < m_{\widetilde{\tau}}$ in light of the expected experimental uncertainties. Indeed, for $m_{\widetilde{a}} \lesssim 1$ GeV, an experimental determination of $m_{\widetilde{a}}$ along (15) will be extremely challenging. Nevertheless, for a given hadronic axion model (i.e., given e_Q and y), the CBBN constraints together with experimental insights into $m_{\widetilde{\tau}}$, $m_{\widetilde{B}}$, $Y_{\widetilde{\tau}}$, and $\Omega_{\rm dm}$ imply new $m_{\widetilde{a}}$-dependent upper limits on the reheating temperature $T_{\rm R}$.[8]

In Fig. 5, we present upper limits on $T_{\rm R}$ imposed by $\Omega_{\widetilde{a}}^{\rm TP} h^2 \leq 0.126$ and by the ^{9}Be CBBN limit on f_a given in Fig. 4, i.e., for $|e_Q| = 1/3$, $m_{\widetilde{B}} = 1.1\, m_{\widetilde{\tau}}$, $Y_{\widetilde{\tau}}$ given by (8), and $y = 1$. The shown limits range from $T_{\rm R}^{\rm max} = 10^5$ GeV up to 10^{10} GeV (as labeled). Once $m_{\widetilde{\tau}}$ is determined at colliders, this figure allows one to infer $(m_{\widetilde{a}}, T_{\rm R})$ combinations that are disfavored by CBBN and $\Omega_{\rm dm}$. The ^{6}Li CBBN limits on f_a are in close vicinity to the ^{9}Be limit, as can be seen in Fig. 4. Thus, we do not show the associated $T_{\rm R}^{\rm max}$ lines since they agree basically with the ones shown in Fig. 5. For $|e_Q| = 1$, $T_{\rm R}^{\rm max}$ becomes less restrictive by almost exactly two orders of magnitude. For example, the $T_{\rm R}^{\rm max} = 10^9$ GeV line for $|e_Q| = 1$ is in close vicinity to the $T_{\rm R}^{\rm max} = 10^7$ GeV line in Fig. 5.

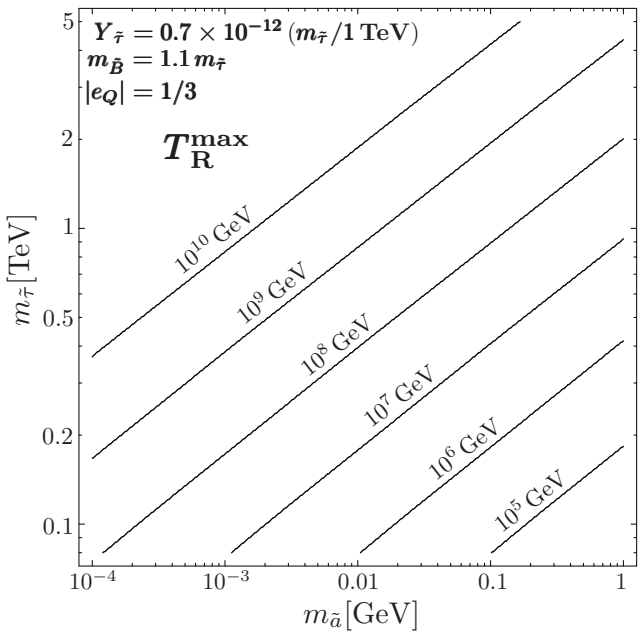

FIG. 5: Upper limits on the reheating temperature $T_{\rm R}$ imposed by $\Omega_{\widetilde{a}}^{\rm TP} h^2 \leq 0.126$ and by the CBBN limit on f_a given by the upper solid line (^{9}Be) in Fig. 4, i.e., for $|e_Q| = 1/3$, $m_{\widetilde{B}} = 1.1\, m_{\widetilde{\tau}}$, $Y_{\widetilde{\tau}}$ given by (8), and $y = 1$.

The obtained upper limits on f_a and $T_{\rm R}$ are conservative ones. For instance, BBN constraints from hadronic energy emitted in 4-body decays $\widetilde{\tau}_{\rm R} \to \tau \widetilde{a} {\rm q}\bar{\rm q}$ can become relevant already for $\tau_{\widetilde{\tau}} \gtrsim 100$ s. These additional constraints—imposed mainly by observationally inferred limits on primordial deuterium—may imply more restrictive f_a limits than obtained here, and thereby $T_{\rm R}^{\rm max}$ values that are more restrictive than the ones in Fig. 5. Effects of late energy injection on ^{6}Li from CBBN have been included in the gravitino LSP case, e.g., in Refs. [48, 49, 50, 51]. The resulting constraints differ only marginally from the ones obtained without taking this effect into account [31, 52, 53].[9] We expect a similar outcome for our CBBN limits and refer the study of constraints from energy injection to a future publication.

[8] Reference [15] also addresses ways to probe $T_{\rm R}$ values but based on $\Omega_{\widetilde{a}}^{\rm TP} + \Omega_{\widetilde{a}}^{\rm NTP} \leq \Omega_{\rm dm}$ and on $\Omega_{\widetilde{a}}^{\rm NTP}$ to be inferred from collider data and without considering BBN constraints in the $\widetilde{a}$ LSP case with a $\widetilde{l}_1$ NLSP, which are the main results of our Letter.

[9] At $t \lesssim 10^3$ s when CBBN is not efficient, injection of energy may have a noticeable effect on the ^{6}Li abundance and could even allow for a solution of the ^{7}Li problem that is consistent with ^{6}Li in the observationally inferred range (13) [49, 54, 55, 56].

VI. DISCUSSION

It has already been realized in Ref. [12] that collider measurements of $\tau_{\widetilde{\tau}}$, $m_{\widetilde{\tau}}$, and $m_{\widetilde{B}}$ will probe the PQ scale f_a in the considered axino LSP scenarios. This is also evident from the results of our 2-loop calculation shown in Fig. 3 and from the associated LL part (7). The f_a value inferred for given e_Q and y can then be used in (2) to extract the $m_{\widetilde{a}}$-dependent limit $T_{\rm R}^{\rm max}$ imposed by $\Omega_{\widetilde{a}}^{\rm TP} \leq \Omega_{\rm dm}$; cf. Fig. 1. However, a $\tau_{\widetilde{\tau}}$ measurement will be challenging from the experimental point of view. In fact, while there are proposals for planned detectors at the International Linear Collider (ILC) [57, 58], new detector concepts may be necessary to stop and collect long-lived $\widetilde{\tau}_1$s for an analysis of their decays [13, 59, 60, 61].

The limits on f_a and $T_{\rm R}$ presented in Figs. 4 and 5 do not rely on a measurement of $\tau_{\widetilde{\tau}}$. They result from upper limits $\tau_{\widetilde{\tau}}^{\rm max}$ imposed by the CBBN constraints,

$$\tau_{\widetilde{\tau}} \leq \tau_{\widetilde{\tau}}^{\rm max} < 10^4\,{\rm s}\ , \tag{16}$$

which show only a very mild dependence on $m_{\widetilde{\tau}}$ for typical yields such as (8); see Fig. 3. In fact, based on (16), it is possible to derive analytic expressions for the upper limits on f_a and $T_{\rm R}$ in a conservative way.

Aiming at an instructive derivation, we work with the LL part (7) which describes $\tau_{\widetilde{\tau}}$ to within 15% accuracy,

$$\tau_{\widetilde{\tau}} \approx \tau_{\widetilde{\tau}\,\rm LL} \equiv \Gamma(\widetilde{\tau}_{\rm R} \to \tau\widetilde{a})^{-1}_{\rm LL} \tag{17}$$

$$\gtrsim \frac{128\pi^5\cos^8\theta_W}{81\,\alpha^4 e_Q^4}\,\frac{f_a^2}{m_{\widetilde{\tau}}\,m_{\widetilde{B}}^2}\,\ln^{-2}\left(\frac{y f_a}{\sqrt{2}m_{\widetilde{\tau}}}\right) \tag{18}$$

$$\gtrsim 3.78\times10^3\ {\rm s}\left(\frac{1/3}{e_Q}\right)^4\left(\frac{f_a}{10^{12}\,{\rm GeV}}\right)^2 \times\left(\frac{100\ {\rm GeV}}{m_{\widetilde{\tau}}}\right)\left(\frac{100\ {\rm GeV}}{m_{\widetilde{B}}}\right)^2, \tag{19}$$

where (18) underestimates $\tau_{\widetilde{\tau}\,\rm LL}$ by at most 2% (15%) for $m_{\widetilde{a}} \lesssim 0.1 m_{\widetilde{\tau}}$ ($m_{\widetilde{a}} \lesssim 0.25 m_{\widetilde{\tau}}$). Focussing on the collider-friendly region $m_{\widetilde{\tau}} \lesssim 1$ TeV, $f_a \lesssim 3\times10^{13}$ GeV is imposed by CBBN for $|e_Q| = 1/3$ and $y = 1$. Based on this and on the LEP bound $m_{\widetilde{\tau}} \gtrsim 80$ GeV, $\ln(y f_a/\sqrt{2}m_{\widetilde{\tau}}) \lesssim 26.3$ is used to get from (18) to (19). Accordingly, $\tau_{\widetilde{\tau}\,\rm LL}$ can be underestimated by (19) by a factor of $\mathcal{O}(1)$ at $f_a \ll 3\times10^{13}$ GeV and/or 80 GeV $\ll m_{\widetilde{\tau}} \lesssim 1$ TeV. Nevertheless, (19) allows us to translate the constraint (16) in a conservative way into the following upper limit:

$$f_a \ \lesssim\ 1.63\times10^{12}\,{\rm GeV}\left(\frac{e_Q}{1/3}\right)^2\left(\frac{\tau_{\widetilde{\tau}}^{\rm max}}{10^4\,{\rm s}}\right)^{1/2} \times\left(\frac{m_{\widetilde{\tau}}}{100\ {\rm GeV}}\right)^{1/2}\left(\frac{m_{\widetilde{B}}}{100\ {\rm GeV}}\right) \equiv f_a^{\rm max}\ . \tag{20}$$

A comparison with the numerically obtained ^{9}Be limits at $m_{\widetilde{a}}^2/m_{\widetilde{\tau}}^2 \ll 1$ shows a good overall agreement for $\tau_{\widetilde{\tau}}^{\rm max} \approx 5\times10^3$ s. The associated analytical expression however is less restrictive (i.e., more conservative) than the numerically obtained limits towards larger $m_{\widetilde{\tau}}$. In fact, there the actual $\tau_{\widetilde{\tau}}^{\rm max}$ value imposed by CBBN becomes more restrictive as can be seen in Fig. 3.

Let us now turn to $T_{\rm R}$ on which a conservative limit

$$T_{\rm R} \lesssim 1.7\times10^6\,{\rm GeV}\left(\frac{\Omega_{\rm dm}h^2}{0.1}\right)\left(\frac{f_a}{10^{11}\,{\rm GeV}}\right)^2\left(\frac{0.1\ {\rm MeV}}{m_{\widetilde{a}}}\right) \tag{21}$$

is imposed by

$$\Omega_{\rm dm}h^2 \geq \Omega_{\widetilde{a}}^{\rm TP}h^2 \tag{22}$$

$$\gtrsim 0.6\left(\frac{10^{11}\,{\rm GeV}}{f_a}\right)^2\left(\frac{m_{\widetilde{a}}}{0.1\ {\rm MeV}}\right)\left(\frac{T_R}{10^7\,{\rm GeV}}\right)\ . \tag{23}$$

Here the constant "conservative" prefactor 0.6 accounts for the $T_{\rm R}$-dependent prefactor in (2), which stays in the range $0.6 < 5.5\,g_{\rm s}^6(T_{\rm R})\ln[1.211/g_{\rm s}(T_{\rm R})] < 1.06$ for $10^4\,{\rm GeV} \leq T_{\rm R} \leq 10^{12}\,{\rm GeV}$ if the MSSM 1-loop renormalization group running of g_s is considered. Using the upper limit (20) in (21), one arrives immediately at an analytic expression for the CBBN-imposed limit,

$$T_{\rm R}\ \lesssim\ 4.4\times10^8\,{\rm GeV}\left(\frac{e_Q}{1/3}\right)^4\left(\frac{\Omega_{\rm dm}h^2}{0.1}\right)\left(\frac{0.1\ {\rm MeV}}{m_{\widetilde{a}}}\right) \times\left(\frac{\tau_{\widetilde{\tau}}^{\rm max}}{10^4\,{\rm s}}\right)\left(\frac{m_{\widetilde{\tau}}}{100\ {\rm GeV}}\right)\left(\frac{m_{\widetilde{B}}}{100\ {\rm GeV}}\right)^2 \equiv T_{\rm R}^{\rm max}\ , \tag{24}$$

which is conservative. For $\tau_{\widetilde{\tau}}^{\rm max} \approx 5\times10^3$ s, we find again a good overall agreement with the limits obtained numerically. However, as expected from its derivation, the associated analytic expression can be by a factor of $\mathcal{O}(1)$ less restrictive than the numerical results shown in Fig. 5.

Since $\tau_{\widetilde{\tau}}$ depends on the ratio f_a/e_Q^2, the limits (20) and (24) depend on e_Q and thus on the specific axion model. It would therefore be particularly valuable to discover the axion and its mass since the relation between m_a and f_a does not depend on e_Q. If f_a can thus be determined, $T_{\rm R}^{\rm max}$ would be given by (21) directly. In addition, one could find e_Q in a $\tau_{\widetilde{\tau}}$ measurement or derive a lower limit on it from the CBBN constraints (16).

In this respect we note that most axion searches probe the axion-photon-coupling $g_{a\gamma\gamma}$ in certain ranges of the axion mass m_a; cf. [6] and references therein. In the models considered [62], $g_{a\gamma\gamma}$ does also depend on f_a and e_Q. An axion discovery at an $(m_a, g_{a\gamma\gamma})$ combination would thus be associated with an (f_a, e_Q) combination in the considered models. The e_Q value from axion searches could then be compared to the one inferred from a $\tau_{\widetilde{\tau}}$ measurement at colliders or, if this is not possible, to its lower limit imposed by CBBN.

The region in which the presented BBN constraints are expected to become relevant is explored by the axion dark matter experiment (ADMX) which searches for resonant conversion of dark matter axions into photons in a microwave cavity [63, 64]. Axion searches of this type are sensitive to $g_{a\gamma\gamma}$ only in the combination $g_{a\gamma\gamma}^2\rho_a$, where ρ_a denotes the local halo density of axions. If axinos

provide the dominant component of cold dark matter, ρ_a can be very small so that no signals will appear at the expected $g_{a\gamma\gamma}$ values. An axion signal in such a direct search would in turn imply a sizeable axion density, $\Omega_a \sim \Omega_{\rm dm}$, and thereby a restrictive $T_{\rm R}$ limit in the considered $m_{\widetilde{a}}$ range, $m_{\widetilde{a}} \gtrsim 0.1$ MeV, given by (21) or (24) with $\Omega_{\rm dm} \to \Omega_{\rm dm} - \Omega_a$. Alternatively, evidence for solar axions could appear in the Tokyo Axion Helioscope or the CERN Axion Solar Telescope (CAST) [65, 66, 67]. This would imply $\Omega_a \ll \Omega_{\rm dm}$, $f_a \lesssim 10^9\,{\rm GeV}$ and thus $T_{\rm R} \ll 10^6\,{\rm GeV}$ in the considered axino cold dark matter scenarios; cf. (21) with $m_{\widetilde{a}} \gtrsim 0.1$ MeV. Here the CBBN constraints will be relevant only in the exceptional cases with $e_Q \to 0$ and/or $m_{\widetilde{a}} \to m_{\widetilde{\tau}}$.

VII. SUMMARY AND CONCLUSIONS

We have explored BBN constraints in axino cold dark matter scenarios with a long-lived charged slepton $\tilde{l}_1$. Calculating the lifetime $\tau_{\tilde{l}_1}$, which is governed by 2-loop diagrams in hadronic axion models, we find that $\tilde{l}_1$ can be sufficiently long lived to allow for an efficient catalysis of ^{6}Li and ^{9}Be via bound-state formation with primordial nuclei. Observationally inferred abundances of ^{6}Li and ^{9}Be thus impose upper limits on $\tau_{\tilde{l}_1}$ for typical thermal relic abundances of the long-lived $\tilde{l}_1$. These limits have allowed us to derive upper limits on the PQ scale f_a that depend mainly on the masses of the slepton, $m_{\tilde{l}_1}$, and the lightest neutralino, $m_{\widetilde{\chi}_1^0}$, and on the electric charge of the heavy (s)quarks e_Q. The obtained f_a constraints imply new upper limits on the reheating temperature $T_{\rm R}$ since f_a governs not only $\tau_{\tilde{l}_1}$ but also the efficiency of thermal axino production and thereby the $T_{\rm R}$ constraints imposed by $\Omega_{\widetilde{a}}^{\rm TP} \leq \Omega_{\rm dm}$. We have presented both numerical results and analytical approximations for those new BBN-imposed limits and have discussed their dependence on $m_{\widetilde{a}}$, $m_{\tilde{l}_1}$, $m_{\widetilde{\chi}_1^0}$, and e_Q. For example, for $m_{\tilde{l}_1} = 500$ GeV, $m_{\widetilde{\chi}_1^0} = 1.1\ m_{\tilde{l}_1}$, and $|e_Q| = 1/3$, we find $f_a \lesssim 10^{13}\,{\rm GeV}$ and that $T_{\rm R} \gtrsim 10^9\,{\rm GeV}$ is viable only for $m_{\widetilde{a}} \lesssim 1$ MeV.

We have addressed the extent to which the BBN-imposed limits on f_a and $T_{\rm R}$ can be probed experimentally if the considered axino LSP scenario is realized. With not too heavy Standard Model superpartners, LHC experiments will allow us to measure $m_{\tilde{l}_1}$ and $m_{\widetilde{\chi}_1^0}$ and to infer the thermal relic $\tilde{l}_1$ abundance prior to decay under the assumption of a standard cosmological history. With the ILC and/or new detector concepts, even a measurement of $\tau_{\tilde{l}_1}$ is conceivable, and our $\tau_{\tilde{l}_1}$ result shows that this could give insights into f_a/e_Q^2. A determination of $m_{\widetilde{a}}$ however seems possible only for relatively heavy axinos $0.1 m_{\tilde{l}_1} \lesssim m_{\widetilde{a}} < m_{\tilde{l}_1}$ and hopeless for $m_{\widetilde{a}}^2/m_{\tilde{l}_1}^2 \ll 1$ [12]. Moreover, insights into e_Q—or, more generally, into the axion model—seem to require not only an axion discovery but a determination of its mass m_a (and thereby of f_a) in axion search experiments.

A simple form of the superpotential has been considered that is generic for SUSY hadronic axion models in which the axion multiplet interacts with the MSSM multiplets through loops of heavy (s)quarks. While we have explored the case with a minimum number of $\mathrm{SU}(2)_{\rm L}$-singlet KSVZ multiplets and with $\tilde{l}_1$ being a purely right-handed stau $\widetilde{\tau}_{\rm R}$, our study can be generalized to more complicated settings in a straightforward way.

Without specifying the SUSY breaking mechanism or other details of the PQ sector, we have assumed saxion effects to be negligible and a spectrum with the $\widetilde{a}$ LSP and the $\tilde{l}_1$ NLSP. Our results depend crucially on these assumptions. In situations in which the saxion dominates the energy density before its decay, the entropy per comoving volume can be enhanced by a factor $\Delta > 1$. If this additional entropy production takes place before $\tilde{l}_1$ decoupling, the BBN constraint on f_a will not be affected but the thermally produced axino density can be diluted so that $\Omega_{\widetilde{a}}^{\rm TP} \to \Omega_{\widetilde{a}}^{\rm TP}/\Delta$ and $T_{\rm R}^{\rm max} \to \Delta T_{\rm R}^{\rm max}$. If entropy increases by a large factor of $\Delta > 10^3$ after $\tilde{l}_1$ decoupling and before BBN, the $\tilde{l}_1$ abundance can be diluted such that catalyzed BBN (CBBN) of ^{6}Li and ^{9}Be cannot become efficient. Then the CBBN-imposed constraints on f_a and $T_{\rm R}$ would not exist. Nevertheless, $\Omega_{\widetilde{a}}^{\rm TP} \to \Omega_{\widetilde{a}}^{\rm TP}/\Delta$ so that the $\Omega_{\rm dm}$-imposed limit on $T_{\rm R}$ would be relaxed by a factor of Δ. However note that the baryon asymmetry would also be diluted by a factor of Δ and therefore a larger asymmetry would be needed before its dilution; see Ref. [37] for a related discussion in the $\widetilde{G}$ LSP case.

The cosmological constraints presented in this work can also be affected by the presence of the gravitino $\tilde{G}$ even for a standard thermal history. Its mass $m_{\tilde{G}}$—which depends on the SUSY breaking mechanism and the SUSY breaking scale—governs the strength of its interactions. The gravitino can be produced thermally in the early Universe, with the resulting abundance depending on $m_{\tilde{G}}$ and T_R [68, 69]. In the scenario studied in this Letter, $m_{\widetilde{a}} < m_{\tilde{l}_1} < m_{\tilde{G}}$, the heavy gravitino is typically long-lived and its decays may affect BBN. Thereby additional constraints on T_R can be incurred [51, 70].

If $m_{\tilde{G}} < m_{\tilde{l}_1}$ and $\Gamma(\tilde{l}_1 \to l\widetilde{a}) \ll \Gamma(\tilde{l}_1 \to l\widetilde{G})$, $\tau_{\tilde{l}_1}$ is governed by $\tilde{l}_1 \to l\widetilde{G}$. Then our f_a limit can be evaded while the CBBN constraints discussed in [31, 37, 49, 51, 52, 53, 71, 72] and their implications for thermally produced gravitino abundance become relevant. On the other hand, if $\Gamma(\tilde{l}_1 \to l\widetilde{a}) \gg \Gamma(\tilde{l}_1 \to l\widetilde{G})$, the CBBN limits discussed in this Letter also apply. However, the gravitinos lead to an increase of the LSP density, thus leading to more restrictive T_R limits. In this case our results remain as conservative upper limits.

Our investigations show that for the interesting case of new long-lived charged particles, BBN constraints play an important role and can be used to restrict the models considerably. These constraints will become particularly important if such particles are produced and detected at the upcoming LHC experiments.

Acknowledgments

We are grateful to Koichi Hamaguchi, Kazunori Nakayama, Josef Pradler, Sabine Schilling, and Fuminobu Takahashi for valuable discussions. NT would like to thank the Max Planck Institute for Physics for their kind hospitality during parts of this work. DW would like to thank SLAC for their kind hospitality during parts of this work. This research was partially supported by the Cluster of Excellence 'Origin and Structure of the Universe' and by the Swiss National Science Foundation (SNF) under contract 20-116756/2.

[1] S.A. Bonometto, F. Gabbiani, A. Masiero, Phys. Rev. **D49**, 3918 (1994), hep-ph/9305237
[2] L. Covi, J.E. Kim, L. Roszkowski, Phys. Rev. Lett. **82**, 4180 (1999), hep-ph/9905212
[3] L. Covi, H.B. Kim, J.E. Kim, L. Roszkowski, JHEP **05**, 033 (2001), hep-ph/0101009
[4] L. Covi, L. Roszkowski, R. Ruiz de Austri, M. Small, JHEP **06**, 003 (2004), hep-ph/0402240
[5] A. Brandenburg, F.D. Steffen, JCAP **0408**, 008 (2004), hep-ph/0405158
[6] F.D. Steffen, Eur. Phys. J. **C59**, 557 (2009), 0811.3347
[7] H. Baer, M. Haider, S. Kraml, S. Sekmen, H. Summy, JCAP **0902**, 002 (2009), 0812.2693
[8] C. Amsler et al. (Particle Data Group), Phys. Lett. **B667**, 1 (2008)
[9] P. Sikivie, Lect. Notes Phys. **741**, 19 (2008), astro-ph/0610440
[10] G.G. Raffelt, J. Phys. **A40**, 6607 (2007), hep-ph/0611118
[11] G.G. Raffelt, Lect. Notes Phys. **741**, 51 (2008), hep-ph/0611350
[12] A. Brandenburg, L. Covi, K. Hamaguchi, L. Roszkowski, F.D. Steffen, Phys. Lett. **B617**, 99 (2005), hep-ph/0501287
[13] K. Hamaguchi, M.M. Nojiri, A. de Roeck, JHEP **03**, 046 (2007), hep-ph/0612060
[14] D.N. Spergel et al. (WMAP), Astrophys. J. Suppl. **170**, 377 (2007), astro-ph/0603449
[15] K.Y. Choi, L. Roszkowski, R. Ruiz de Austri, JHEP **04**, 016 (2008), 0710.3349
[16] M. Kawasaki, K. Nakayama, M. Senami, JCAP **0803**, 009 (2008), 0711.3083
[17] J.E. Kim, Phys. Rev. Lett. **67**, 3465 (1991)
[18] D.H. Lyth, Phys. Rev. **D48**, 4523 (1993), hep-ph/9306293
[19] S. Chang, H.B. Kim, Phys. Rev. Lett. **77**, 591 (1996), hep-ph/9604222
[20] M. Hashimoto, K.I. Izawa, M. Yamaguchi, T. Yanagida, Phys. Lett. **B437**, 44 (1998), hep-ph/9803263
[21] M. Fukugita, T. Yanagida, Phys. Lett. **B174**, 45 (1986)
[22] S. Davidson, A. Ibarra, Phys. Lett. **B535**, 25 (2002), hep-ph/0202239
[23] W. Buchmüller, P. Di Bari, M. Plümacher, Ann. Phys. **315**, 305 (2005), hep-ph/0401240
[24] S. Blanchet, P. Di Bari, JCAP **0703**, 018 (2007), hep-ph/0607330
[25] S. Antusch, A.M. Teixeira, JCAP **0702**, 024 (2007), hep-ph/0611232
[26] J.E. Kim, Phys. Rev. Lett. **43**, 103 (1979)
[27] M.A. Shifman, A.I. Vainshtein, V.I. Zakharov, Nucl. Phys. **B166**, 493 (1980)
[28] J.E. Kim, Phys. Lett. **B136**, 378 (1984)
[29] M. Pospelov, Phys. Rev. Lett. **98**, 231301 (2007), hep-ph/0605215
[30] M. Pospelov (2007), 0712.0647
[31] M. Pospelov, J. Pradler, F.D. Steffen, JCAP **0811**, 020 (2008), 0807.4287
[32] M. Beltran, J. Garcia-Bellido, J. Lesgourgues, Phys. Rev. **D75**, 103507 (2007), hep-ph/0606107
[33] K. Rajagopal, M.S. Turner, F. Wilczek, Nucl. Phys. **B358**, 447 (1991)
[34] F.D. Steffen, JCAP **0609**, 001 (2006), hep-ph/0605306
[35] T. Asaka, T. Yanagida, Phys. Lett. **B494**, 297 (2000), hep-ph/0006211
[36] M.E. Gomez, S. Lola, C. Pallis, J. Rodriguez-Quintero, JCAP **0901**, 027 (2009), 0809.1859
[37] J. Pradler, F.D. Steffen, Phys. Lett. **B648**, 224 (2007), hep-ph/0612291
[38] E. Braaten, T.C. Yuan, Phys. Rev. Lett. **66**, 2183 (1991)
[39] A. Freitas, F.D. Steffen, N. Tajuddin, D. Wyler (2009), in preparation
[40] F. Jegerlehner, Nucl. Phys. Proc. Suppl. **181-182**, 135 (2008), 0807.4206
[41] L. Covi, L. Roszkowski, M. Small, JHEP **07**, 023 (2002), hep-ph/0206119
[42] T. Asaka, K. Hamaguchi, K. Suzuki, Phys. Lett. **B490**, 136 (2000), hep-ph/0005136
[43] M. Ratz, K. Schmidt-Hoberg, M.W. Winkler, JCAP **0810**, 026 (2008), 0808.0829
[44] J. Pradler, F.D. Steffen, Nucl. Phys. **B809**, 318 (2009), 0808.2462
[45] M. Kamimura, Y. Kino, E. Hiyama (2008), 0809.4772
[46] R.H. Cyburt, J.R. Ellis, B.D. Fields, K.A. Olive, Phys. Rev. **D67**, 103521 (2003), astro-ph/0211258
[47] M. Asplund, D.L. Lambert, P.E. Nissen, F. Primas, V.V. Smith, Astrophys. J. **644**, 229 (2006), astro-ph/0510636
[48] K. Jedamzik, JCAP **0803**, 008 (2008), 0710.5153v2
[49] R.H. Cyburt, J.R. Ellis, B.D. Fields, K.A. Olive, V.C. Spanos, JCAP **0611**, 014 (2006), astro-ph/0608562
[50] M. Kawasaki, K. Kohri, T. Moroi, Phys. Lett. **B649**, 436 (2007), hep-ph/0703122
[51] M. Kawasaki, K. Kohri, T. Moroi, A. Yotsuyanagi, Phys. Rev. **D78**, 065011 (2008), 0804.3745
[52] J. Pradler, F.D. Steffen, Phys. Lett. **B666**, 181 (2008), 0710.2213
[53] J. Pradler, F.D. Steffen, Eur. Phys. J. **C56**, 287 (2008), 0710.4548
[54] K. Jedamzik, Phys. Rev. **D70**, 063524 (2004), astro-ph/0402344
[55] K. Jedamzik, K.Y. Choi, L. Roszkowski, R. Ruiz de Austri, JCAP **0607**, 007 (2006), hep-ph/0512044v2
[56] S. Bailly, K. Jedamzik, G. Moultaka (2008), 0812.0788
[57] H.U. Martyn, Eur. Phys. J. **C48**, 15 (2006), hep-ph/0605257
[58] H.U. Martyn (2007), 0709.1030
[59] J.L. Goity, W.J. Kossler, M. Sher, Phys. Rev. **D48**, 5437

(1993), hep-ph/9305244
[60] K. Hamaguchi, Y. Kuno, T. Nakaya, M.M. Nojiri, Phys. Rev. **D70**, 115007 (2004), hep-ph/0409248
[61] J.L. Feng, B.T. Smith, Phys. Rev. **D71**, 015004 (2005), hep-ph/0409278
[62] J.E. Kim, Phys. Rev. **D58**, 055006 (1998), hep-ph/9802220
[63] L.D. Duffy et al., Phys. Rev. **D74**, 012006 (2006), astro-ph/0603108
[64] G. Carosi, K. van Bibber, Lect. Notes. Phys. **741**, 135 (2008), hep-ex/0701025
[65] S. Andriamonje et al. (CAST), JCAP **0704**, 010 (2007), hep-ex/0702006
[66] J. Ruz et al., J. Phys. Conf. Ser. **110**, 062023 (2008)
[67] M. Minowa et al. (2008), 0809.0596
[68] M. Bolz, A. Brandenburg, W. Buchmüller, Nucl. Phys. **B606**, 518 (2001), hep-ph/0012052
[69] J. Pradler, F.D. Steffen, Phys. Rev. **D75**, 023509 (2007), hep-ph/0608344
[70] K. Kohri, T. Moroi, A. Yotsuyanagi, Phys. Rev. **D73**, 123511 (2006), hep-ph/0507245
[71] F.D. Steffen, AIP Conf. Proc. **903**, 595 (2007), hep-ph/0611027
[72] F.D. Steffen, Phys. Lett. **B669**, 74 (2008), 0806.3266